

ESTIMATION OF THE FREQUENCY RANGE OF LEAST REACTIVE POWER FOR A SINGLE-PHASE TRANSFORMER

K. Moessner^{1*}, J. Kremer¹ and T. Leibfried¹

¹ Institute of Electric Energy Systems and High Voltage Technology,
Karlsruhe Institute of Technology, Kaiserstrasse 12, 76131 Karlsruhe, Germany

*Email: kai.moessner@kit.edu

Abstract: This paper presents a simple transformer model, established to simulate the steady-state operation of single-phase core-type and shell-type transformers under no-load condition. This work aims to set up a simple method to estimate active, reactive and apparent power during induced voltage tests on single-phase transformers. Different amplitudes and frequencies of the fundamental of the test voltage can be evaluated in order to find a possible frequency range of least reactive power. This transformer model incorporates basic topology, dimensions and material data of the magnetic core, the coupling between the electric and magnetic circuit and the major capacitances within the transformer. The comparison between simulation results and laboratory measurements on a single-phase testing transformer is presented.

1 INTRODUCTION

According to international standards [1], [2] induced voltage tests are part of the dielectric routine tests for almost all types of liquid-immersed and dry-type distribution and power transformers. Induced voltage tests have to be conducted on transformers to prove alternating voltage withstand capability of the insulation along the windings, the insulation between different phases of the winding systems and the insulation between the line terminals and connected windings to ground and the other winding systems. In [3] and [4] test procedure information for short and long duration induced voltage tests on liquid-immersed transformers is provided: Depending on the number of phases and the highest voltage of equipment U_m , the requirements, test connection diagrams, test methods, duration and practice, the required test voltage levels with their respective dwell time, the need for partial discharge measurement and the interpretation of the results are specified for single-phase and three-phase transformers with uniformly or non-uniformly insulated windings. Furthermore [3] demands the alternating voltage for single or three-phase excitation to be sinusoidal to the greatest possible extent; frequency has to be raised sufficiently above rated frequency to avoid core saturation, since test voltage levels are higher than the rated voltage levels of the devices under test (DUT). Reference [4] specifies a minimum test frequency to be exceeded, depending on the ratio of the induced test voltage across the winding and the rated voltage across the winding. Hence the ratio volts per hertz and the flux density in the core are limited to 110 % of the rated values, as demanded in [2]. Often certain predetermined frequencies are chosen as default frequencies of the fundamental of the test voltage, especially for fixed speed motor-generator-sets. Rotary converters with

variable speed and especially test systems powered by static frequency converters offer the opportunity to individually adjust the test frequency. In [5] and [6] the consumed reactive and apparent power of different transformers under no load condition are sketched for different amplitudes and frequencies of the fundamental of the test voltage. Each of the examined transformers shows a frequency range, in which the consumed apparent and reactive power is minimal. In combination with the application of additional compensating reactors these characteristics can be used to minimize the current to be provided by the voltage source for induced voltage test, as in particular for very high test voltages the demand for capacitive reactive power can reach enormous levels [6]. Position and width of this frequency range, as well as the dependency on the applied voltage level and the absolute value of measured power is different for various transformers and can be related to the effective capacitances within the transformer, to transformer design and to the properties of the used material especially concerning the transformer core [6]. In [7] a method to calculate the load for the induced voltage test is presented: Therefore the test circuit is simplified to a R-L-C parallel oscillation circuit, whose estimated power consumption can be calculated: First a determination of the prevailing magnetic induction during the test procedure in dependence of the ratio of the test frequency and the test voltage to their respective rated values has to be conducted. In combination with the specific magnetizing apparent power and specific iron losses as a function of induction and frequency of the applied voltage, apparent and active power can be determined by multiplication with the total mass of electrical steel, leading to the inductive component of reactive power by vectorial subtraction. Capacitive reactive power can be estimated by a simple approximate formula for two-

winding transformers, using the capacitance between high voltage and ground C_E and U_{diff} , the highest voltage difference across C_E [7]

$$Q_{kap} = -\frac{C_E \cdot \omega \cdot U_{diff}^2}{3} \quad (1)$$

This paper discusses the attempt to refine the load calculation in [7], enabling the estimation of the characteristics presented in [5] and [6] for single-phase transformers by applying a qualified single-phase transformer model.

2 SINGLE-PHASE TRANSFORMER MODEL

From a variety of proceedings for transformer modeling the approach used for the present examinations is based on an analytical mathematical description of the coupling between electric and magnetic circuitry and an incorporation of the nonlinear effects introduced by the transformer core, i.e. magnetic hysteresis, saturation and eddy current effects, as presented in [8]. For the present investigations models for shell-type and core-type single-phase transformers have been established. Due to the later comparison between simulation results and laboratory measurements the following considerations and equations in this paper are given for single-phase shell-type topology, but are also valid for core-type topology.

2.1 Equivalent circuit

The underlying equivalent circuit shown in Figure 1 includes a three-legged transformer core with the cross sections A_{c1} , A_{c2} and A_{c3} , the mean length of the magnetic paths l_{c1} , l_{c2} , l_{c3} and the fluxes Φ_1 , Φ_2 and Φ_3 . Furthermore the voltages at the terminals $u_1(t)$ and $u_2(t)$, the number of turns N_1 and N_2 , winding resistance R and leakage inductance L of the primary and secondary winding are taken into account. Eddy current effects are considered by insertion of the nonlinear resistance R_e . As a simple approach the various capacitances between primary winding and ground and between secondary winding and ground are merged to the capacitances C_1 and C_2 . The effective capacitance between primary and secondary windings is

considered as lumped capacitance C_3 . R_3 and the load resistor R_L are inserted for the simulation due to stability reasons. The coupling between electric circuit and magnetic circuit is realized by relating the time derivatives of the flux linkages and the time derivatives of the winding currents using expressions for self inductances and mutual inductances of the windings. These can be calculated using N_1 and N_2 and the incremental permeability $\mu_d = dB/dH$ of the electrical steel.

2.2 Hysteresis modeling

As electrical steel used for transformer cores is a ferromagnetic material, the hysteresis-shaped dependence of magnetic flux density B and prevailing magnetic field H must not be disregarded. From a large number of descriptions for the magnetic hysteresis the widely used macroscopic model according to D. C. Jiles and D. L. Atherton [9] has been chosen for this study, taking into account the underlying physics of material characteristics. Its advantages are its easy implementation by first-order differential equations using only five parameters, whose determination is possible by analyzing measured hysteresis loops.

$$M_{an}(H) = M_S \cdot \left[\coth\left(\frac{H + \alpha \cdot M}{a}\right) - \frac{a}{H + \alpha \cdot M} \right] \quad (2)$$

expresses anhysteretic magnetization of ideal material without defects using the Langevin equation, comprising the augmentation of the applied magnetic field strength by aM , representing interdomain coupling with the mean field parameter α . a is characterizing the shape of the anhysteretic magnetization, M_S is the saturation magnetization. Due to the superposition of reversible and irreversible magnetization effects for real material, the bulk magnetization M can be decomposed into its irreversible and reversible component. The irreversible magnetization process M_{irr} is considered by setting up the differential equation

$$\frac{dM_{irr}}{dH} = \frac{M_{an} - M_{irr}}{k \cdot \delta - \alpha \cdot (M_{an} - M_{irr})}, \quad (3)$$

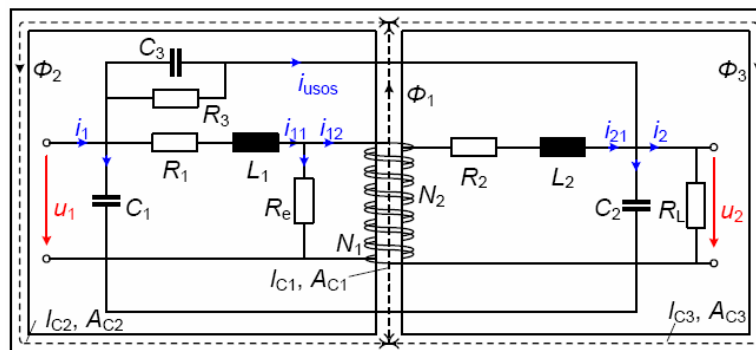


Figure 1: Equivalent circuit of a single-phase shell-type transformer

using $\delta = \text{sign}(dH/dt)$ and the pinning coefficient k . The reversible component of magnetization M_{rev} is

$$M_{rev} = c \cdot (M_{an} - M_{irr}) \quad (4)$$

with the proportionality factor c . Incremental permeability now can be formulated to

$$\mu_d = \mu_0 \left(1 + \frac{dM_{rev}}{dH} + \frac{dM_{irr}}{dH} \right), \quad (5)$$

where μ_0 is the vacuum permeability.

2.3 Winding parameters

Winding resistances are composed of d.c. resistances obtainable by measurement of the winding resistance according to [1] and [4] and an a.c. component to account for eddy current losses, stray losses, proximity effect [11] and skin effect [12]. Total winding resistance can be approximated as given in [13] by

$$R = R_{DC} + R_{EC} \cdot \left(\frac{f}{f_0} \right)^m \quad (6)$$

with $1.2 \leq m \leq 2$ being a frequency dependent factor itself. Ref [13] proposes to use $m = 2$. R_{EC} can be determined during load loss measurement: The additional amount of resistance for a.c. excitation can be placed at primary and secondary winding side to a different extend or, as first approach, be portioned equally [8].

The total leakage inductance can be determined by measurement of short-circuit impedance; the division among the winding systems is arbitrary for two-winding transformers [12]. Reference [12] advices to assume concentric winding design and to put 75 % to 90 % of total inductance on high voltage side in contrast to [8], dividing total leakage inductance equally on high- and low-voltage side.

In opposite to [8], where any capacitances are neglected, [11] and [12] suggest, that transformer winding and bushing capacitances are of critical importance to slow transient resonance phenomena. Therefore manufacturer data or at least typical values listed in the literature have to be used; assuming cylindrical configuration of the windings the capacitances can be treated as cylindrical capacitors, whose capacitance can be calculated using available design information. Alternatively the effective capacitances can be measured at the terminals of the windings.

2.4 Core Parameters

Total transformer loss is made up from iron core losses, dielectric losses and winding losses, the latter two being of negligible interest under no-load

condition. Iron core losses are commonly separated into hysteresis losses P_h , classical eddy current losses P_{cl} and excess losses or anomalous losses P_{exc} [10]. In ferromagnetic laminations during one cycle of magnetization the amount of energy per unit volume of

$$w_{Fe} = \oint_B H dB = A_{Hys} \quad (7)$$

is transformed into heat, corresponding with the area of the hysteresis loop A_{Hys} [14]. Total losses can be determined by multiplication with the volume V of the specimen and the magnetization frequency f ,

$$P_{total} = A_{Hys} \cdot f \cdot V. \quad (8)$$

Empirical examinations confirm the total power losses being proportional to the maximum flux density $P_{total} \sim B_{max}^{1.7}$ [10] and the frequency $P_{total} \sim f^{1.6}$ [15].

The hysteresis loss is associated with the amount of energy being dissipated during magnetization by Barkhausen domain wall jumps and irreversible domain rotation processes. As the consumed energy in these processes can be regarded independent of magnetization frequency, the hysteresis power losses are classified as static losses and can be determined by evaluation of the area of the direct current hysteresis loop $A_{Hys,DC}$ [14]: The following empirical equation, proposed by Steinmetz in 1892, relates the hysteresis power losses to frequency and flux density [14]

$$P_{Hys} = K_{Hys} \cdot f \cdot B^n. \quad (9)$$

There are several instances in literature [10, 14] specifying typical values for the Steinmetz exponent n ranging between 1.5 and 2.5; as an approximation it can be selected $n = 2$.

In contrast to static losses, which occur due to the discontinuous character of the magnetization processes at a microscopic scale [10], the calculation of the losses according to the classical eddy current approach assumes a uniform magnetization. A periodic change of flux density induces a voltage and due to a limited resistivity in the core an eddy current is driven. According to [8, 10, 14] the power loss dissipated per unit volume by eddy currents can be calculated to

$$P_{Cl} = \frac{(\pi \cdot d \cdot B_{max} \cdot f)^2 \sigma}{6} \quad (10)$$

for a sinusoidal excitation, considering the thickness of the lamination d and the conductivity σ of the material. The classical model neglects the

skin effect and assumes an uniform field distribution and the thickness being significantly less than the width of the lamination. However the sum of the values of calculated hysteresis losses and eddy current losses is significantly less than corresponding measured losses; the difference is called anomalous loss or excess loss. It appears as in ferromagnetic material the microscopic magnetization is not homogenous and the classical eddy current loss calculation does not consider local eddy currents induced by microscopic change of magnetization due to domain wall moving [10, 14]. Excess losses can be as large or larger as the classical eddy current losses and rise with increasing domain size [14]. For a sinusoidal voltage supply the excess losses per unit volume are given by

$$P_{exc} = 8 \cdot (\sigma \cdot G \cdot \tau \cdot d \cdot H_0)^{0.5} \cdot (B_{max} \cdot f)^{1.5} \quad (11)$$

using the material constants G and H_0 and the width of the lamination τ .

For transformer modeling in the time domain the total iron losses can be represented by an equivalent resistance R_e inserted in parallel to the primary winding. Generally R_e can be chosen linear or nonlinear and can be calculated using material properties and dimensions of the electrical steel lamination: For the examinations presented in this paper R_e can be derived from equations (9), (10) and (11). A transformer core modeling should take into account the intrinsic properties and intrinsic quality of the core material as they result from material measurements on test samples e.g. in Epstein frames or single sheet testers. For transformer modeling these losses have to be augmented due to a large number of factors considering the core design and construction: Depending on joint types, number of sheets per stack, local saturation in the vicinity of joints, rotating fields in the vicinity of T-joints, clamping stress impact and the deterioration of the material during manufacturing due to stacking holes, punching and slitting, etc. [16, 17] the losses increase. Hence it is customary to define a building factor as the ratio

$$K_b = \frac{P_{total}}{P_{total} \text{ predicted by test specimen}}, \quad (12)$$

which can reach values up to 1.1 [17] or 1.15 to 1.2 [16]. For this work K_b was set to an arbitrary value $K_b = 1.16$ between the empirically specified limits in [16].

The absolute value of apparent power can be calculated by multiplying the rms values of primary current and applied voltage; vectorial subtraction of apparent power and power losses leads to the absolute value of reactive power.

3 REALIZATION

Laboratory measurements have been conducted on a 75 kVA single-phase testing transformer to validate the transformer model.

3.1 Transformer Data

The number of windings on primary and secondary side, the used core material as well as the cross section area of the yoke and the side limbs, the cross section of the central wound limb and the effective magnetic path lengths through the central and side limbs could be extracted from manufacturer specifications. D.c. winding resistance has been determined according to [1]; the measurement of relative short-circuit impedance has been conducted having low-voltage side short-circuited and mains voltage applied to the high voltage side. 75 % of total leakage inductance has been put on high voltage side, the additional winding resistance R_{EC} in respect to equation (6) has been equally allocated to primary and secondary winding. The effective terminal winding capacitances between high voltage and low voltage winding, between high voltage winding and ground and between low voltage winding and ground were measured using a Schering-bridge. As mentioned before, an ohmic resistor $R_3 = 1 \text{ G}\Omega$ has been inserted in parallel to the capacitance between high- and low-voltage side and an ohmic resistor R_2 has been inserted at the terminals of the secondary winding to simulate insulation conductivity and to eliminate stability issues during simulation. In contrast to experiential values resistance had to be decreased to $R_2 = 70 \text{ M}\Omega$ for the latter reason.

3.2 Core Data

The density $\rho = 7650 \text{ kg/m}^3$ and the electrical conductivity $\sigma = 2.083 (\mu\Omega\text{m})^{-1}$ of the used grain-oriented electrical steel type M165-35 S are taken from literature listings [18]. The thickness of the electrical steel sheet is $d = 0.35 \text{ mm}$. Epstein frame measurements have been conducted according to [19] on test specimen of comparative core material, producing DC- and 50-Hz-AC hysteresis loops, which, amongst others, provide the values for the total iron losses per unit mass at $f = 50 \text{ Hz}$, the hysteresis loss per cycle per unit volume and a basis for the determination of the parameters for hysteresis modeling as presented above. These parameters have been determined according to [20]. Additionally mathematical optimization methods have been used to find alternative sets of parameters representing the core material.

4 RESULTS

4.1 Hysteresis

Figure 2 shows the 50-Hz-hysteresis loops for the

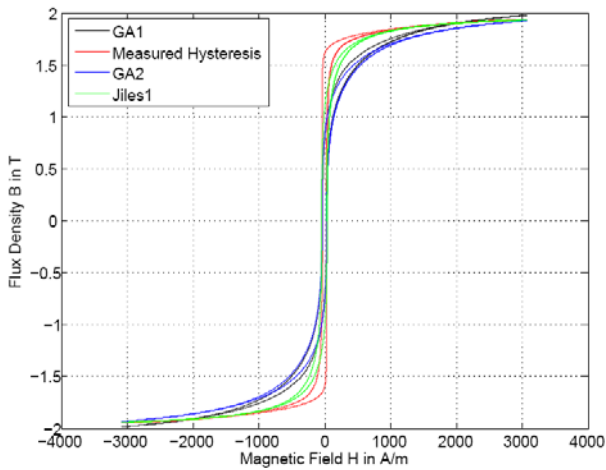


Figure 2: Hysteresis: Measurement and simulation

core material as measured by means of an Epstein frame (red) and modeled using the method proposed in [9]: The set of parameters “Jiles1” leading to the green hysteresis has been determined using manual modification of the result of the approach introduced in [20]; the alternative sets of parameters, with which the black and blue hysteresis curves were generated, have been acquired using an genetic algorithm (GA) to minimize the sum of squared residuals. As shown in Figure 2 the simulated magnetization curves do not entirely match the measured hysteresis. Therefore deviations between calculated and measured values of the losses, apparent power and reactive power are inevitable. Hence measured quantities are inserted into equations (9), (10) and (11) to calculate total power loss per unit volume, depending on the chosen frequency and the simulated maximum magnetic flux density in the core. Total power losses can then be obtained by a multiplication with the core volume more precisely than by averaging the product of the instantaneous values of voltage and current at the primary winding terminals.

4.2 Electrical Quantities

To produce plausible results, the cross section area of the transformer core, taken as basis for calculation, has to be reduced compared to the dimensions specified by the manufacturer: Due to design and construction of the core, flux density is not likely to be distributed uniformly in the entire core. As the available construction data is not detailed enough for extensive considerations, including FEM evaluation of the non-uniform flux distribution in the corners and joints of the core, an effective core cross-section area of 93 % of the actual value has been assumed carrying uniform magnetic flux density, leaving 7 % of the actual core without flux. Additionally the modeled bulk capacitance between primary winding and ground had to be augmented by the factor $1.2 \cdot 10^4$ to obtain any capacitive influence expected to appear for increasing the frequency of the applied voltage.

Taking account for these assumptions, the voltage and current at the primary winding terminals are sketched in Figure 3 for rated amplitude and frequency of the fundamental of the voltage: Simulation results for the sets of model parameters associated with the hysteresis curves in Figure 2 are opposed to the current measured during operation of the transformer at laboratory mains. The impact of different model parameters on the wave shape of the current can be seen as well as the deviation from measurement due to the inaccurate hysteresis modeling.

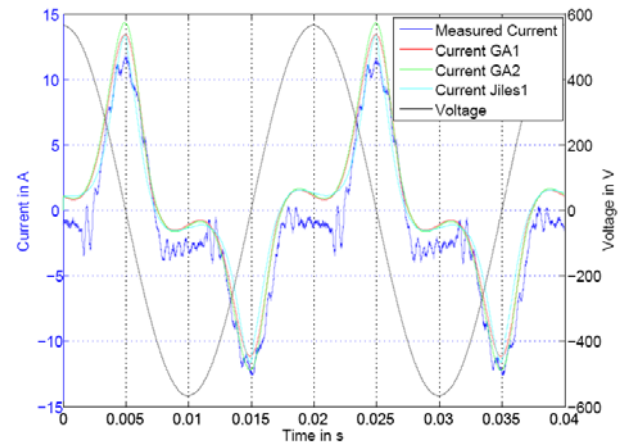


Figure 3: Voltage and Current at the terminals of primary winding: Measurement and simulation

The values of power for operation with an excitation voltage of 75 %, 87.5 % and 100 % of rated voltage U_r and different frequencies of the fundamental have been calculated for different sets of parameters. The best matching between simulations and measurement results could be produced for a set of Jiles-Atherton parameters obtained by application of genetic algorithms. In Figure 4 these simulation results are set in contrast to the corresponding values of apparent and reactive power and power losses, which have been measured at the terminals of the existing transformer, making use of a single-phase static

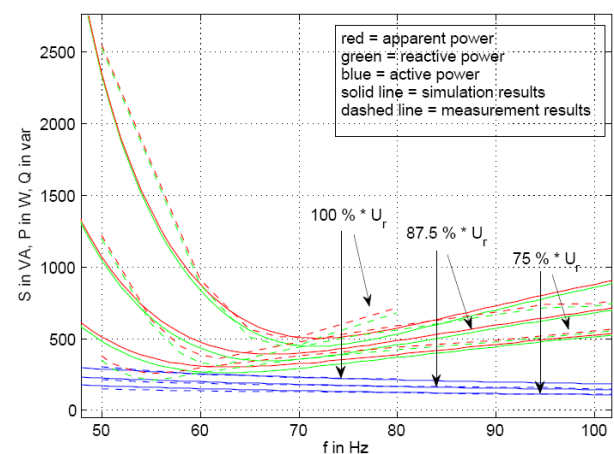


Figure 4: Power: Measurement and simulation

frequency converter and a matching transformer. The occurring difference increases for decreasing voltage level. This can be ascribed to the insufficient congruence between measured and modeled hysteresis, which is worsening for reduced levels of excitation.

5 CONCLUSION

A simple model for single-phase transformers has been established to estimate power losses, apparent and reactive power for different amplitudes and frequencies of the fundamental of the voltage applied during induced voltage test, in order to identify a possible frequency range of least reactive power. This model is based on an analytical description of a simple transformer equivalent circuit, incorporating the nonlinear magnetic properties of the core. Magnetic hysteresis has been modeled according to the approach of D. C. Jiles and D. L. Atherton. Due to the insufficient congruence to the measured hysteresis, simulation results are feasible, but do not completely match the results obtained from measurements on an existing single-phase transformer, which have been conducted to validate the model.

6 REFERENCES

- [1] IEC 60076-1, Power transformers, Part 1: General, 1993
- [2] IEEE Standard for General Requirements for Liquid-Immersed Distribution, Power and Regulating Transformers, IEEE Std C57.12.00, 2010
- [3] IEC 60076-3, "Power transformers – Part 3: Insulation levels, dielectric tests and external clearances in air", 2000
- [4] IEEE Standard Test Code for Liquid-Immersed Distribution, Power and Regulation Transformers, IEEE Std C57.12.90, 2010
- [5] K. Moessner, T. Leibfried, M. Gamlin, "Alternating Voltage Tests on Distribution Transformers Using Static Frequency Converters", in Proc. of the 16th International Symposium on High Voltage Engineering, Cape Town, South Africa, August 24th – 28th, 2009
- [6] A. Thiede, T. Steiner, R. Pietsch, "New Approach of testing Power Transformers by Means of Static Frequency Converters", CIGRE Session, Paris, France, August 23th – 27th, 2010
- [7] A. Carlson, J. Fuhr, G. Schemel, F. Wegscheider, "Testing of Power Transformers and Shunt Reactors", 2nd Edition, ABB Ltd, Transformers, 2010
- [8] A. D. Theocharis, J. Miliadis-Argitis, Th. Zacharias, "Single-phase transformer model including magnetic hysteresis and eddy currents", Electrical Engineering, Volume 90, Number 3, pp. 229–241, 2008
- [9] D. C. Jiles, D. L. Atherton, "Theory of Ferromagnetic Hysteresis", Journal of Magnetism and Magnetic Materials, Volume 61, pp. 48-60, 1986
- [10] G. Bertotti, "General properties of power losses in soft ferromagnetic materials", IEEE Transactions on Magnetics, Volume 24, pp. 621–630, 1988
- [11] B. Mork et al., "Hybrid Transformer Model for Transient Simulation – Part I: Development and Parameters", IEEE Transactions on Power Delivery, Volume 22, pp. 248-255, 2007
- [12] J. A. Martinez, "Parameter Determination for Modeling System Transients – Part III: Transformers", IEEE Transactions on Power Delivery, Volume 20, pp. 2051-2062, 2005
- [13] E. F. Fuchs, D. Yildirim, and W. M. Grady, "Measurement of Eddy-current Loss Coefficient P_{EC-R} , derating of Single-Phase Transformers, and Comparison with K-factor Approach," IEEE Transactions on Power Delivery, Volume 15, pp. 148–154, 2000.
- [14] Z. Neuschl, "Rechnerunterstützte experimentelle Verfahren zur Bestimmung der lastunabhängigen Eisenverluste in permanentmagnetisch erregten elektrischen Maschinen mit additionalem Axialfluss", PhD Thesis, Brandenburgische Technische Universität Cottbus, 2007
- [15] R. Fischer, "Elektrische Maschinen", Hanser Fachbuchverlag, 2006
- [16] M. Elleuch, M. Poloujadoff, "Analytical Model of Iron Losses in Power Transformers", IEEE Transactions on Magnetics, Volume 39, pp. 973–980, 2003
- [17] H. Akcay, D. G. Ece, "Modeling of Hysteresis and Power Losses in Transformer Laminations", IEEE Transactions on Power Delivery, Volume 18, pp. 487-492, 2003
- [18] Orb Electrical Steels Ltd, "Electrical Steel, Grain Oriented, Unisil, Unisil-H", Product Brochure, 2002
- [19] IEC 60404-2, "Magnetic materials – Part 2: Methods of measurement of the magnetic properties of electrical steel strip and sheet by means of an Epstein frame", 1996
- [20] D. C. Jiles, J. B. Thielke, M. K. Devine, "Numerical Determination of Hysteresis Parameters for the Modeling of Magnetic Properties Using the Theory of Ferromagnetic Hysteresis", IEEE Transactions on Magnetics, Volume 28, pp. 27–35, 1992